

# Sharp finite statistics for quantum key distribution

Vaisakh Mannalath<sup>1,2,3,\*</sup>, Víctor Zapatero<sup>1,2,3,\*</sup> and Marcos Curty<sup>1,2,3</sup>

<sup>1</sup>*Vigo Quantum Communication Center, University of Vigo, Vigo E-36310, Spain*

<sup>2</sup>*Escuela de Ingeniería de Telecomunicación, Department of Signal Theory and Communications, University of Vigo, Vigo E-36310, Spain and*

<sup>3</sup>*AtlantTic Research Center, University of Vigo, Vigo E-36310, Spain*

The performance of quantum key distribution (QKD) heavily depends on statistical inference. For a broad class of protocols, the central statistical task is a random sampling problem, customarily addressed using exponential tail bounds on the hypergeometric distribution. Here we devise a strikingly simple exponential bound for this task, of unprecedented tightness among QKD security analyses. As a by-product, confidence intervals for the average of non-identical Bernoulli parameters follow too. These naturally fit in statistical analyses of decoy-state QKD and also outperform standard tools. Lastly, we show that, in a vast parameter regime, the use of tail bounds is not enforced because the cumulative mass function of the hypergeometric distribution is accurately computable. This sharply decreases the minimum block sizes necessary for QKD, and reveals the tightness of our simple analytical bounds when moderate-to-large blocks are considered.

*Introduction.* Quantum key distribution (QKD) is the only approach to key exchange that is provably secure against computationally unbounded adversaries [1]. Today, considerable efforts are being made to boost the performance of practical QKD systems while guaranteeing their physical-layer security [2, 3]. Among the multiple facets of this ongoing program, it is of utmost importance to achieve tighter lower bounds on the extractable secret key length, a goal that can be tackled by refining QKD security proofs. These proofs build upon quantum information-theoretic results and strongly rely on statistical inference, which plays a pivotal role to keep the necessary data block sizes to a minimum.

To be precise, establishing the finite-key security of a QKD protocol requires to upper bound the probability of a “failure” happening in its parameter estimation (PE) step. This refers to the event where the protocol does not abort but the adversary obtains non-trivial information about the final key [1]. In BB84-like protocols [4], a very popular proof technique is based on an entropic uncertainty relation (EUR) for smooth entropies [5, 6], in which case the simplest formulation of the problem goes as follows. Let us consider a two-piece experiment where a population of  $N$  binary random variables is generated according to an arbitrary probability distribution, and a random sample of size  $n$  is drawn from the population afterwards. If we denote the frequency of ones in the test (complementary) sample as  $\hat{p}$  ( $\hat{q}$ ), the goal is to find a threshold value  $q^{\text{th}} \geq p^{\text{th}}$  such that

$$\Pr\left[\hat{p} \leq p^{\text{th}}, \hat{q} \geq q^{\text{th}}\right] \leq \epsilon, \quad (1)$$

for arbitrary values of  $N$ ,  $n$ ,  $\epsilon$  and  $p^{\text{th}}$ . Naturally, an interplay exists between  $\epsilon$  and  $q^{\text{th}}$ : fulfilling Eq. (1) with a

very small  $\epsilon$  comes at the price of tolerating larger values of  $q^{\text{th}}$ . In the context of QKD—in which  $\hat{q}$  is often referred to as the phase-error rate (PHER)—this translates into a direct penalty on the provably secure key length. Notably, the above formulation of the problem shows up exactly in ideal implementations of the BB84 [4] or the BBM92 [7, 8] protocols, and we adhere to the latter in the main text for didactic purposes. The detailed protocol description and the secret key length formula can be found in Supplemental Material I. On the other hand, the popular decoy-state BB84 protocol [9–12], which is implemented in most of today’s commercial QKD setups, is addressed in Supplemental Material II.

In EUR-based security proofs [8, 13], it is commonplace to derive the desired  $q^{\text{th}}$  by resorting to an exponential tail bound on the hypergeometric (HG) distribution known as Serfling inequality [14]. Recently though, a sharper bound has been derived in [15], combining Serfling inequality with a refined inequality due to Hush and Scovel [16]. Nonetheless, the attainable improvement is moderate and heavily relies on the use of very large samples for testing, an undesirable feature given the fact that the final key is extracted from the complementary data.

In this paper, we propose a simpler approach to calculate  $q^{\text{th}}$ , resorting to a well-known link between random sampling with and without replacement [17]. Remarkably, the bound we obtain outperforms [15] in all the explored parameter regimes relevant for QKD. Furthermore, in the derivation of the bound, confidence intervals (CIs) are obtained for the average parameter of a set of independent Bernoulli trials. These intervals, which provide an additional tool required for current decoy-state QKD security proofs, also outperform the analytical results considered for that purpose so far [12, 18]. Lastly, we show that, contrary to general belief, the cumulative mass function (CMF) of the HG distribution is exactly computable in a vast parameter regime of interest to QKD. Crucially, this enables the calculation of optimal—so-called Clopper-Pearson—one-sided CIs for the population parameter [19]. Ap-

\* These authors contributed equally to this paper.  
vmannalath@vqcc.uvigo.es  
vzapatero@vqcc.uvigo.es

plying the latter to the random sampling problem of Eq. (1)—and also to its generalization to decoy-state QKD schemes—we report a dramatic decrease of the minimum block sizes necessary for key extraction. On the other hand, explicit comparison with our simple analytical tools reveals the tightness of the latter for moderate-to-large blocks.

*Analytical results.* Our analytical results are triggered by two observations. First, the additive Chernoff bound [20], conventionally used in the context of sampling with replacement, also holds for sampling without replacement. This feature, which is a consequence of a more general theorem by Hoeffding [17]—see also [21] for a simple proof—has already been exploited in QKD security analyses before [22, 23]. Secondly, regardless of the context, very loose relaxations of the bound are often used in the literature. With this in mind, we derive a tight relaxation of the additive Chernoff bound and indistinctly use it to obtain one-sided CIs for the population parameters in sampling with and without replacement. Then, we apply these CIs to address the problem of Eq. (1) and its generalization to decoy-state QKD.

Crucially, our relaxation stems from a rational approximation of the Kullback-Leibler divergence, which is based on a logarithmic inequality [24] carefully selected to keep the CIs tight and handy at the same time. Indeed, higher-order rational approximations of the logarithm lead to much more convoluted formulas for the divergence. The reader is referred to Supplemental Material III for the relaxed Chernoff bound, and the corresponding CIs are stated in Proposition 1 and Corollary 1 below.

**Proposition 1.** *Let  $\hat{p}$  be the average of  $n$  independent Bernoulli variables, with expected value  $\mathbb{E}[\hat{p}] = p$ , and let  $\kappa_{n,\epsilon} = (2/9n) \ln(1/\epsilon)$ . Then, for all  $\epsilon > 0$ ,  $\Pr[\Gamma_{n,\epsilon}^-(\hat{p}) \geq p] \leq \epsilon$  and  $\Pr[\Gamma_{n,\epsilon}^+(\hat{p}) \leq p] \leq \epsilon$ , where*

$$\Gamma_{n,\epsilon}^-(\hat{p}) = \begin{cases} \gamma_{n,\epsilon}^-(\hat{p}) & \text{if } \hat{p} \in \left[\frac{3\kappa_{n,\epsilon}}{1+\kappa_{n,\epsilon}}, 1\right], \\ -\epsilon & \text{otherwise,} \end{cases} \quad (2)$$

$$\Gamma_{n,\epsilon}^+(\hat{p}) = \begin{cases} \gamma_{n,\epsilon}^+(\hat{p}) & \text{if } \hat{p} \in \left[0, \frac{1-2\kappa_{n,\epsilon}}{1+\kappa_{n,\epsilon}}\right], \\ 1+\epsilon & \text{otherwise,} \end{cases} \quad (3)$$

and

$$\gamma_{n,\epsilon}^\pm(x) = \frac{1}{1+4\kappa_{n,\epsilon}} \left[ 3\kappa_{n,\epsilon} + (1-2\kappa_{n,\epsilon})x \pm 3\sqrt{\kappa_{n,\epsilon}(\kappa_{n,\epsilon} + x - x^2)} \right]. \quad (4)$$

A proof of this claim is given in Supplemental Material III. Importantly, since the claim is solely derived from the additive Chernoff bound, it automatically extends to a HG random variable [17, 21]. The upper extension goes as follows.

**Corollary 1.** *Let  $\hat{X} \sim \text{Hypergeometric}(N, K, n)$  and  $\hat{p} = \hat{X}/n$ , such that  $\mathbb{E}[\hat{p}] = p$  with  $p = K/N$ . Then, for all  $\epsilon > 0$ ,  $\Pr[\Gamma_{n,\epsilon}^+(\hat{p}) \leq p] \leq \epsilon$ , where  $\Gamma_{n,\epsilon}^+(x)$  is defined in Proposition 1.*

This result readily implies the following proposition.

**Proposition 2.** *A test sample of size  $n$  is drawn at random from a binary population with  $N$  elements. Let  $\hat{p}$  ( $\hat{q}$ ) denote the frequency of ones in the test (complementary) sample. For all  $\epsilon > 0$ ,*

$$\Pr[\hat{q} \geq q_{N,n,\epsilon}^{\text{th}}(\hat{p})] \leq \epsilon \quad (5)$$

for

$$q_{N,n,\epsilon}^{\text{th}}(x) = \frac{N\Gamma_{n,\epsilon}^+(x) - nx}{N - n}, \quad (6)$$

where  $\Gamma_{n,\epsilon}^+(x)$  is defined in Proposition 1.

*Proof.* Let  $\hat{X}$  be the number of ones in the test sample, such that  $\hat{p} = \hat{X}/n$ . If we denote by  $p$  the fraction of ones in the population,  $\hat{X} \sim \text{Hypergeometric}(N, Np, n)$  and the claim follows directly from Corollary 1 by substituting  $p = n\hat{p}/N + (N-n)\hat{q}/N$  and rearranging terms.  $\square$

As shown next, Proposition 2 allows to obtain a threshold value  $q^{\text{th}}$  fulfilling Eq. (1), in so providing the failure probability estimation of the BBM92 protocol.

**Proposition 3.** *Consider the two-piece experiment presented in the Introduction. Then, for all  $\epsilon > 0$  and  $p^{\text{th}} < 1/2$ ,*

$$\Pr[\hat{p} \leq p^{\text{th}}, \hat{q} \geq q_{N,n,\epsilon}^{\text{th}}(p^{\text{th}})] \leq \epsilon \quad (7)$$

for the threshold function  $q_{N,n,\epsilon}^{\text{th}}(x)$  defined in Eq. (6), given that the latter is locally non-decreasing at  $p^{\text{th}}$ .

*Proof.* Let  $\hat{T}$  denote the frequency of ones occurring in the population. Then,

$$\begin{aligned} \Pr[\hat{p} \leq p^{\text{th}}, \hat{q} \geq q_{N,n,\epsilon}^{\text{th}}(p^{\text{th}})] &\leq \Pr[\hat{q} \geq q_{N,n,\epsilon}^{\text{th}}(\hat{p})] \\ &\leq \sum_p \Pr[\hat{T} = p] \Pr[\hat{q} \geq q_{N,n,\epsilon}^{\text{th}}(\hat{p}) | \hat{T} = p] \leq \epsilon. \end{aligned} \quad (8)$$

In the first inequality we use the fact that  $\{\hat{p} \leq p^{\text{th}}, \hat{q} \geq q_{N,n,\epsilon}^{\text{th}}(p^{\text{th}})\} \implies \{\hat{q} \geq q_{N,n,\epsilon}^{\text{th}}(\hat{p})\}$ . This is so because  $q_{N,n,\epsilon}^{\text{th}}(x)$  is non-decreasing for  $x \in [0, p^{\text{th}}]$  if it is non-decreasing at  $x = p^{\text{th}}$ , and the latter is guaranteed by assumption. The averaging over  $\hat{T}$  in the second inequality is a purely ad hoc step aimed at enabling the use of Proposition 2, which presumes a fixed frequency of ones in the population. The third inequality follows from Proposition 2.  $\square$

A relevant observation is that the condition on the slope at  $p^{\text{th}}$ , which is equivalent to  $\Gamma_{n,\epsilon}^{+\prime}(p^{\text{th}}) \geq n/N$  ( $\Gamma_{n,\epsilon}^{+\prime}(p^{\text{th}})$  denoting the derivative of  $\Gamma_{n,\epsilon}^+(x)$  with respect to  $x$  evaluated in  $p^{\text{th}}$ ), is unrestrictive for all practical purposes [25].

On another note, the reader is referred to Supplemental Material II for the failure probability estimation of a decoy-state QKD protocol, which relies not only on Proposition 2 but also on Proposition 1.

*Numerical results.* Certainly, tighter results can be obtained by resorting to numerical methods. For instance, using Stirling's formula and the Gaussian cumulative density function, the authors of [22] construct a HG tail inequality that outperforms our relaxed Chernoff bound in certain regimes, but does not enable a closed formula for the related CI. Alternatively, one could use the exact additive Chernoff bound rather than a relaxation. Note, however, that if one is willing to use numerical techniques, tail inequalities may become superfluous. This is so because, contrary to general belief, accurately computing the CMF of the HG distribution is often feasible in QKD applications. Crucially, this enables the calculation of the strictest possible one-sided CIs [26, 27] using the well-known Clopper-Pearson method based on pivoting the CMF [19]. In particular, for our purposes, one can replace  $\Gamma_{n,\epsilon}^+(\hat{p})$  in Corollary 1 by the tighter statistic  $\mathcal{CP}_{N,n,\epsilon}^+(\hat{p})$ , defined via [27]

$$\mathcal{CP}_{N,n,\epsilon}^+(x) = \min \{p \geq x \mid \Pr[\hat{p} \leq x \mid p] \leq \epsilon\} \quad (9)$$

if the target set of the minimization is non-empty, and  $\mathcal{CP}_{N,n,\epsilon}^+(x) = (N+1)/N$  otherwise [28], where we recall that  $p$  takes discrete values in the set  $\{0, 1/N, 2/N, \dots, 1\}$  [29]. Remarkably, accurate determination of the CMF is required in order to compute  $\mathcal{CP}_{N,n,\epsilon}^+(\hat{p})$ , with a numerical precision beyond  $\epsilon$  according to Eq. (9). Indeed, for a broad range of settings of interest to QKD, this is a manageable task with existing software.

Importantly, since  $\mathcal{CP}_{N,n,\epsilon}^+(\hat{p})$  fulfills Corollary 1, it also fulfills Proposition 2, and monotonicity considerations allow to further establish Proposition 3 replacing Eq. (6) by

$$q_{N,n,\epsilon}^{\text{th}}(x) = \frac{N\mathcal{CP}_{N,n,\epsilon}^+(x) - nx}{N - n}. \quad (10)$$

In Fig. 1 we compare the candidate threshold values  $q^{\text{th}}$  satisfying Eq. (1): Eq. (6), Eq. (10), and the thresholds derived in [15] and [8]. For illustration purposes, we consider typical QKD inputs,  $p^{\text{th}} \leq 4\%$ ,  $N = 10^5$ ,  $n = 10^4$  and  $\epsilon = 10^{-9}$ , and remark that the improvement of our tools —*i.e.* Eq. (6) and Eq. (10)— prevails in all the explored parameter regimes relevant for QKD.

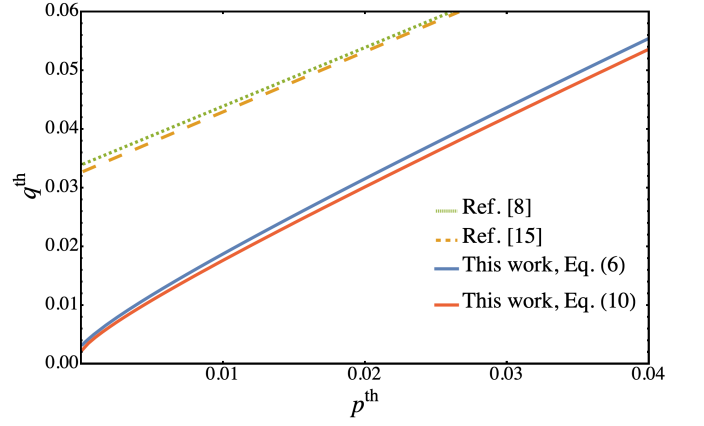


Figure 1: Threshold value  $q^{\text{th}}$  satisfying Eq. (1), for  $p^{\text{th}} \leq 4\%$ ,  $N = 10^5$ ,  $n = 10^4$  and  $\epsilon = 10^{-9}$ . The solid red (blue) line corresponds to our numerical (analytical) tool, based on the exact cumulative mass function of the hypergeometric distribution (a relaxed additive Chernoff bound [20]). The dashed orange line uses the result in [15], which combines Serfling [14] and Hush & Scovel [16] inequalities, and the dotted green line uses the result in [8], based on Serfling inequality alone.

On another note, in Supplemental Material IV we include optimal one-sided CIs for the average of independent Bernoulli parameters [30, 31], potentially replacing  $\Gamma_{n,\epsilon}^+(\hat{p})$  (Proposition 1) in the failure probability estimation of decoy-state QKD schemes. These CIs are related to the well-known Clopper-Pearson CIs of the binomial distribution, which in fact have been used in the context of QKD security before (see e.g. [32, 33]).

*QKD simulations.* Next, we show the impact that the proposed tools have in the finite-key performance of QKD. Let us consider the ideal BBM92 protocol first. Consistently with [8, 15], we evaluate a simplified scenario in which Alice and Bob share a  $2N$ -partite quantum state as a protocol input. Then, they jointly select between two binary and complementary quantum measurements uniformly at random on a round-by-round basis, in so each of them extracting a raw data block of  $N$  bits. These blocks are randomly splitted into a fixed-length test (sifted-key) string of  $n$  ( $N - n$ ) bits. That is to say, both the key and the test string are randomly sampled from the two bases. In the simulations, we set the tolerated quantum bit error rate (QBER) to  $p^{\text{th}} = 4.55\%$  for ease of comparison with [15], where this choice is motivated by the results of the Micius experiment [34]. Also, an error correction (EC) leakage of  $\lambda_{\text{EC}} = 1.19(N - n)h(p^{\text{th}})$  bits is assumed,  $h(x)$  denoting the binary entropy of  $x$ . The correctness parameter,  $\epsilon_{\text{cor}}$ , and the privacy amplification error,  $\epsilon_{\text{PA}}$ , are both set to  $10^{-8}$  for illustration purposes, and the failure probability bound is set to  $\epsilon_{\text{PE}} = 4 \times 10^{-16}$ . Altogether, these settings lead to an overall secrecy parameter of  $\epsilon_{\text{sec}} \approx 5 \times 10^{-8}$  (see Supplemental Material I).

With these inputs, in Fig. 2a we plot the extractable key length divided by the data block size for blocks up to  $N = 10^6$  bits, optimizing the sampling fraction  $n/N$ . In addition, we superpose an inset of the minimum block-size regime, showing that our analytical tool (solid blue line) allows to reduce the minimum block size with respect to [15] (dashed orange line) by more than 16%, while our numerical tool (solid red line) attains a reduction beyond 40%. Furthermore, the tool of [15] would roughly require a three-orders-of-magnitude larger  $\epsilon_{PE}$  for a nonzero key with the block size collected in the Micius experiment [34], indicated with a dotted red vertical line in the inset. Notably as well, both of our tools perform very similarly—and significantly above [8, 15]—for non-critical block sizes.

Let us now assess the more practical decoy-state BB84 protocol. We consider a scheme with three common intensities per basis,  $\mu$  (signal),  $\nu$  (decoy) and  $\omega$  (vacuum), and employ the  $Z$  ( $X$ ) basis for key extraction (PE) with a fixed-size data block of  $N_Z$  ( $N_X$ ) bits drawn at random from the corresponding data pool. Again, in the simulations we contemplate blocks up to  $N = N_Z + N_X = 10^6$  bits, and superpose an inset of the minimum block-size regime. Naturally, we set  $N_Z = q_Z^2/(q_Z^2 + q_X^2)N$ , where  $q_Z$  ( $q_X$ ) denotes the  $Z$  ( $X$ ) basis probability, common to both parties. Also, while we fix  $\omega = 10^{-4}$  to account for the finite extinction ratio of the intensity modulator [35], the settings  $\mu$  and  $\nu$ , together with their respective probabilities,  $p_\mu$  and  $p_\nu$ , and the test basis probability,  $q_X$ , are tuned to optimize the key length per block,  $l/N$ . For simplicity, in order to select the acceptance thresholds of the PE tests [36], the average behaviour of a typical fiber and detector model is considered (see Supplemental Material II for further details). We assume an overall system loss of 30 dB, a dark count probability of  $p_d = 6 \times 10^{-7}$  [37], and a misalignment error rate of  $e_{mis} = 5 \times 10^{-3}$  [12]. As in the BBM92 protocol, the EC leakage is set to  $\lambda_{EC} = 1.19N_Z h(\theta^{th})$ ,  $\theta^{th}$  denoting the correctable QBER of a key block [38]. Lastly, we set again the overall failure probability to  $\epsilon_{PE} = 4 \times 10^{-16}$ , and assume a common value for each individual error term contributing to it [39]. Similarly, we take  $\epsilon_{cor} = \epsilon_{PA} = \delta = 10^{-8}$ , where  $\delta > 0$  is an intrinsic variable of the security analysis (see Supplemental Material II). Overall, this leads to  $\epsilon_{sec} = 7 \times 10^{-8}$ .

The results are shown in Fig. 2b. Unlike the BBM92 protocol, the finite-key security of the decoy-state scheme does not rely on the random sampling tool alone, but also on CIs for the average parameter of a set of Bernoulli trials. Indeed, such CIs are repeatedly used in the decoy-state analysis, and thus they have a very critical impact in the performance. As an example, both orange lines in Fig. 2b use the random sampling tool of [15], but the dotted line relies on Hoeffding inequality [17] for the extra CIs (as originally done in [12]), while the dashed one relies on the multiplicative Chernoff bound [20] (following the improvement of [18]). Meanwhile, the solid blue line results from using the

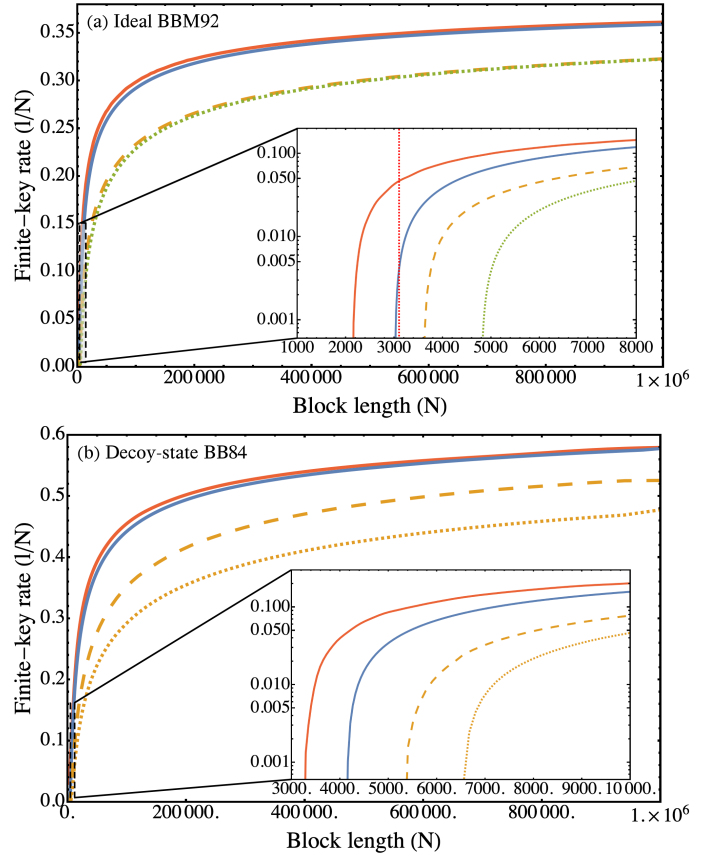


Figure 2: Finite secret key rate versus data block size. (a) Ideal BBM92 protocol. The solid red (blue) line corresponds to our numerical (analytical) tool, the dashed orange line uses the result in [15], and the dotted green line uses the result in [8]. The dotted red vertical line in the inset indicates the block size gathered in the Micius experiment [34],  $N = 3100$  bits. (b) Decoy-state BB84 protocol. The same color code is used again, indicating the random sampling tool under consideration (in particular, the approach of [8] is not presented in this case). The additional confidence intervals required for the decoy-state analysis are selected as specified in the main text. For both figures, the settings employed in the simulations are provided in the main text as well.

random sampling tool of Proposition 2 and the extra CIs of Proposition 1, both originating from our relaxed additive Chernoff bound and each providing an advantage on its own. Lastly, the solid red line uses our numerical upgrades of these two propositions, deploying optimal CIs in both cases. Overall, our analytical tools reduce the minimum block size by more than 22% compared to previous approaches, and the reduction exceeds 38% with the numerical tools. Once more, our analytical and numerical solutions perform very similarly in non-critical regimes, with a strong edge over existing approaches.

*Conclusions.* The performance of QKD is deeply affected by finite statistics. In satellite QKD [34, 40–42], the data collection per satellite overpass is limited, and sharp statistics may translate into an enormous saving of time and resources. What is more, one could envision future QKD applications requiring short keys on-demand for daily transactions with high security standards. For these, a poor statistical analysis could result in an unbearable penalty.

In this work, we have developed simple analytical tools of unprecedented tightness among EUR-based QKD security proofs [5]. Technically, the key enablers of these tools are a careful relaxation of the long-known additive Chernoff bound [20], and a classical link between random sampling with and without replacement [17]. Arguably, the tools might be of interest beyond the realm of QKD, in applications such as quality control tests, clinical trials or hypothesis testing in general. On top of it, we have put forward the possibility of replacing tail inequalities —the cornerstone of statistical analyses in QKD today— by exact computational methods in statistical inference. Remarkably, our results reveal the game-changing potential of such methods to achieve

QKD with minimum block sizes, and reinforce the tightness of our simpler analytical tools when moderate-to-large blocks are considered.

*Acknowledgements.* We acknowledge fruitful discussions with Jay Bartroff, Davide Rusca and Jean-Daniel Bancal. This work was supported by the Galician Regional Government (consolidation of Research Units: AtlantTIC), the Spanish Ministry of Economy and Competitiveness (MINECO), the Fondo Europeo de Desarrollo Regional (FEDER) through the grant No. PID2020-118178RB-C21, MICIN with funding from the European Union NextGenerationEU (PRTR-C17.I1) and the Galician Regional Government with own funding through the “Planes Complementarios de I+D+I con las Comunidades Autónomas” in Quantum Communication, the European Union’s Horizon Europe Framework Programme under the Marie Skłodowska-Curie Grant No. 101072637 (Project QSI) and the project QSNP (grant agreement No. 101114043). M.C. acknowledges support from a “Salvador de Madariaga” grant from the Spanish Ministry of Science, Innovation and Universities (grant No. PRX22/00192).



## I. APPENDIX I: IDEAL BBM92 PROTOCOL

### A. Protocol description

In this section we describe the ideal BBM92 protocol from Ref. [15], where no detection losses are considered and both the key string and the test string are randomly sampled from the two bases. In this scheme, Alice and Bob agree on the protocol inputs specified in Table I, *i.e.* the parameters  $N, n, p^{\text{th}}, \lambda_{\text{EC}}, \epsilon_{\text{PE}}, \epsilon_{\text{cor}}$ , and  $\epsilon_{\text{PA}}$ . Moreover, they share a  $2N$ -partite quantum state and consistently choose between two complementary measurements on a round-by-round basis, sacrificing a random subset of  $n$  measurement outcomes for testing.

The protocol runs as follows:

1. *Measurement*: Alice and Bob measure their quantum states with two complementary measurements, which they select jointly in each round, obtaining a raw data block of size  $N$ . A sifted key string of length  $N - n$  is sampled at random, and the rest of the raw data (*i.e.*  $n$  bits) constitutes the test string.
2. *Parameter estimation* (PE): They publicly reveal the test data and compute the quantum bit error rate (QBER). If the QBER exceeds a tolerated threshold value  $p^{\text{th}}$ , they abort the protocol.
3. *Error correction* (EC): They run a pre-defined EC protocol to reconcile their sifted keys, revealing  $\lambda_{\text{EC}}$  secret-key bits at most.
4. *Error verification* (EV): They perform an EV step based on 2-universal hashing, using tags of  $\log(2/\epsilon_{\text{cor}})$  bits at most. If the EV tags do not match, they abort the protocol. Otherwise, they proceed to privacy amplification.
5. *Privacy amplification* (PA): The parties perform a PA step based on 2-universal hashing, each of them obtaining a final key of  $l$  bits, with

$$l = \left\lfloor (N - n) \{1 - h[q_{N,n,\epsilon_{\text{PE}}}^{\text{th}}(p^{\text{th}})]\} - \lambda_{\text{EC}} - \log\left(\frac{1}{2\epsilon_{\text{cor}}\epsilon_{\text{PA}}^2}\right) \right\rfloor. \quad (11)$$

Here,  $h(x)$  is the binary entropy function, and the threshold function  $q_{N,n,\epsilon_{\text{PE}}}^{\text{th}}(x)$  depends on the random sampling tool used for PE. These are included in the next section. On the other hand,  $\lambda_{\text{EC}}$  is the EC leakage,  $\epsilon_{\text{cor}}$  is the correctness parameter and  $\epsilon_{\text{PA}}$  is the PA error.

Importantly, this approach yields provably  $(2\sqrt{\epsilon_{\text{PE}}} + \epsilon_{\text{PA}})$ -secret and  $\epsilon_{\text{cor}}$ -correct output keys in virtue of a PA lemma for the smooth min-entropy [43], where  $\epsilon_{\text{PE}}$  denotes the corresponding smoothing parameter. As shown in [8],  $\epsilon_{\text{PE}}$  directly provides an upper bound on the failure probability of the protocol, precisely addressed in the next section.

### B. Failure probability

We recall that, in the BBM92 protocol above, a PE failure refers to the joint event where the PE test succeeds and the presumed threshold on the phase-error rate (PHER) is incorrect [8, 15]. The threshold  $q_{N,n,\epsilon_{\text{PE}}}^{\text{th}}(p^{\text{th}})$  on the PHER can be tuned to guarantee that the failure probability of the protocol is below  $\epsilon_{\text{PE}}$ . Namely, it can be chosen to enforce  $\Pr[\hat{p} \leq p^{\text{th}}, \hat{q} \geq q_{N,n,\epsilon_{\text{PE}}}^{\text{th}}(p^{\text{th}})] \leq \epsilon_{\text{PE}}$ , where  $\hat{p}$  and  $\hat{q}$  respectively denote the QBER and the PHER. Below we provide suitable candidates for the threshold function based on different statistical tools.

Table I: BBM92 protocol inputs

$N$	Raw data block size
$n$	Test data block size
$p^{\text{th}}$	Threshold value for the QBER
$\lambda_{\text{EC}}$	Error correction leakage
$\epsilon_{\text{PE}}$	Failure probability of the parameter estimation step
$\epsilon_{\text{cor}}$	Failure probability of the error correction step
$\epsilon_{\text{PA}}$	Failure probability of the privacy amplification step

### 1. Relaxed additive Chernoff bound

From Proposition 3 in the main text, we have

$$q_{N,n,\epsilon_{\text{PE}}}^{\text{th}}(p^{\text{th}}) = \frac{N\Gamma_{n,\epsilon_{\text{PE}}}^+(p^{\text{th}}) - np^{\text{th}}}{N - n}, \quad (12)$$

where  $\Gamma_{n,\epsilon_{\text{PE}}}^+(x)$  is given in Proposition 1 of the main text. This corresponds to the solid blue line of Fig. 2a there.

### 2. Serfling and Hush & Scovel inequalities combined

From Lemma 1 in [15], we have

$$q_{N,n,\epsilon_{\text{PE}}}^{\text{th}}(p^{\text{th}}) = \max_{\xi} \left\{ p^{\text{th}} + \xi + \frac{1}{N - n} \sqrt{1 + \frac{1}{2g} \ln \left[ \frac{1}{\epsilon_{\text{PE}} - \exp \left( -\frac{2Nn\xi^2}{N - n + 1} \right)} \right]} \right\} \quad (13)$$

with

$$g = \frac{1}{N(p^{\text{th}} + \xi) + 1} + \frac{1}{N(1 - p^{\text{th}} - \xi) + 1}, \quad (14)$$

where the maximization runs over all  $\xi > 0$  such that  $N(p^{\text{th}} + \xi) \in \mathbb{Z}^+$  and  $\epsilon_{\text{PE}} > \exp \left( -\frac{2Nn\xi^2}{N - n + 1} \right)$ .

As mentioned in the main text, this approach provides an optimized combination of Serfling inequality [14] with Hush and Scovel inequality [16], and it corresponds to the dashed orange line of Fig. 2a in the main text.

### 3. Serfling inequality

Using Lemma 6 from [8] (which follows from Serfling inequality [14]), we have

$$q_{N,n,\epsilon_{\text{PE}}}^{\text{th}}(p^{\text{th}}) = p^{\text{th}} + \sqrt{\frac{N(n+1) \ln(\epsilon_{\text{PE}}^{-1})}{2(N-n)n^2}}. \quad (15)$$

This corresponds to the dotted green line of Fig. 2a in the main text.

### 4. Exact hypergeometric cumulative mass function

In the main text, a numerical confidence upper bound  $\mathcal{CP}_{N,n,\epsilon}^+(\hat{p})$  on the population parameter is presented [27], based on the classical Clopper-Pearson method of pivoting the cumulative mass function [19]. Since one can replace  $\Gamma_{n,\epsilon}^+(\hat{p})$  by  $\mathcal{CP}_{N,n,\epsilon}^+(\hat{p})$  in Corollary 1 of the main text,  $\mathcal{CP}_{N,n,\epsilon}^+(\hat{p})$  automatically fulfills Proposition 2 there as well. From this, one can easily show that it also satisfies Proposition 3, thereby providing another suitable threshold function:

$$q_{N,n,\epsilon_{\text{PE}}}^{\text{th}}(p^{\text{th}}) = \frac{N\mathcal{CP}_{N,n,\epsilon_{\text{PE}}}^+(p^{\text{th}}) - np^{\text{th}}}{N - n}. \quad (16)$$

This corresponds to the solid red line in of Fig. 2a in the main text.

## II. APPENDIX II: DECOY-STATE BB84 PROTOCOL

We consider a typical decoy-state BB84 protocol in the lines of [12]. Particularly, three common intensities are used in each basis, and the  $Z$  ( $X$ ) basis is employed for key extraction (PE).

### A. Protocol description

Alice and Bob agree on the protocol inputs  $T, q_X, \mathcal{K} := \{\mu, \nu, \omega\}, p_\mu, p_\nu, N_X, N_Z, \theta^{\text{th}}, \lambda_{\text{EC}}, \epsilon_{\text{PE}}, \epsilon_{\text{cor}}, \epsilon_{\text{PA}},$  and  $\delta$ , specified in Table II. In addition, unless the random sampling tool of [15] is considered, they further agree on two more protocol inputs inherent to the corresponding PE test,  $n_{1,Z}^{\text{th}}$  and  $\phi_{1,Z}^{\text{th}}$ . Alternatively, if the tool of [15] is considered, the additional protocol inputs are  $n_{1,Z}^{\text{th,U(L)}}, n_{1,X}^{\text{th,U(L)}},$  and  $m_{1,X}^{\text{th,U}}$ , with which they can ultimately define the relevant threshold values entering the secret key length formula:

$$n_{1,Z}^{\text{th}} = n_{1,Z}^{\text{th,L}}, \quad \phi_{1,Z}^{\text{th}} = \max_{u,v \in \mathcal{B}} q_{u,v,\epsilon_{\text{PE}}}^{\text{th}}(e_{1,X}^{\text{th}}), \quad (17)$$

where  $e_{1,X}^{\text{th}} = m_{1,X}^{\text{th,U}}/n_{1,X}^{\text{th,L}}, \mathcal{B} = \{u \in [n_{1,Z}^{\text{th,L}} + n_{1,X}^{\text{th,L}}, n_{1,Z}^{\text{th,U}} + n_{1,X}^{\text{th,U}}], v \in [n_{1,X}^{\text{th,L}}, n_{1,X}^{\text{th,U}}], u > v\}$ , and the threshold function under consideration is that of Eq. (13). Importantly, we adopt a finer-grained PE test for the random sampling tool of [15] in order to simplify the task of bounding the failure probability in Sec. II C 2 below. Indeed, it is unclear whether a bound can be derived with this tool without modifying the PE test at all. After all, the tool in [15] is devised for the BBM92 protocol specifically, rather than for a decoy-state BB84 protocol, and in this work we provide a possible adaptation to the latter.

The protocol runs as follows. For  $i = 1, \dots, T$ , steps 1 and 2 below are repeated.

1. *State preparation*: Alice chooses a bit value  $y_i$  uniformly at random, a basis setting  $a_i \in \{Z, X\}$  with probability  $q_{a_i}$ , and an intensity setting  $k_i \in \{\mu, \nu, \omega\} =: \mathcal{K}$  with probability  $p_{k_i}$ . She prepares a phase-randomized weak coherent pulse (PRWCP) encoded with the above settings and sends it through the quantum channel to Bob.
2. *Measurement*: Bob measures the incident pulse in the basis  $b_i \in \{Z, X\}$  with probability  $q_{b_i}$ . He records the measurement outcome as  $y'_i \in \{0, 1, \emptyset\}$ , where  $\emptyset$  refers to the “no-click” event. Multiple clicks are assigned to 0 or 1 uniformly at random.

The post-processing and the public discussion run as follows:

3. *Sifting*: The bases and intensity settings are publicly revealed and Alice and Bob identify the sets  $\mathcal{Z} = \{i : a_i = b_i = Z, y'_i \neq \emptyset\}$  and  $\mathcal{X} = \{i : a_i = b_i = X, y'_i \neq \emptyset\}$ .  $N_Z$  rounds are drawn at random from  $\mathcal{Z}$  to form the sifted key data,  $\mathcal{Z}^{\text{sift}}$ , which decomposes as  $\mathcal{Z}^{\text{sift}} = \cup_{k \in \mathcal{K}} \mathcal{Z}_k^{\text{sift}}$  with  $\mathcal{Z}_k^{\text{sift}} = \{i \in \mathcal{Z}^{\text{sift}} : k_i = k\}$ , of size  $n_{Z,k}$ .  $N_X$  rounds are drawn at random from  $\mathcal{X}$  to form the test data,  $\mathcal{X}^{\text{test}}$ , which decomposes as  $\mathcal{X}^{\text{test}} = \cup_{k \in \mathcal{K}} \mathcal{X}_k^{\text{test}}$  with  $\mathcal{X}_k^{\text{test}} = \{i \in \mathcal{X}^{\text{test}} : k_i = k\}$ , of size  $n_{X,k}$ .
4. *Parameter estimation (PE)*: For each  $k \in \mathcal{K}$ , they disclose the bit values in  $\mathcal{X}_k^{\text{test}}$  and compute the corresponding numbers of bit errors,  $m_{X,k}$ . With the available data, they perform the PE test that matches their preferred random sampling tool (see Sec. II C for the details). If the test fails, they abort the protocol.
5. *Error correction (EC)*: They run a pre-defined EC protocol to reconcile their sifted keys, revealing  $\lambda_{\text{EC}}$  secret key bits at most.
6. *Error verification (EV)*: They perform an EV step based on 2-universal hashing, using tags of  $\log(2/\epsilon_{\text{cor}})$  bits at most. If the EV tags do not match, they abort the protocol. Otherwise, they proceed to privacy amplification.
7. *Privacy amplification (PA)*: The parties perform a PA step based on 2-universal hashing, in so obtaining final keys of length

$$l = \left\lfloor n_{1,Z}^{\text{th}} [1 - h(\phi_{1,Z}^{\text{th}})] - \lambda_{\text{EC}} - \log \left( \frac{1}{2\epsilon_{\text{cor}}\epsilon_{\text{PA}}^2\delta} \right) \right\rfloor. \quad (18)$$

This approach yields provably  $[2(\sqrt{\epsilon_{\text{PE}}} + \delta) + \epsilon_{\text{PA}}]$ -secret [43, 44] and  $\epsilon_{\text{cor}}$ -correct keys for the requested failure probability bound,  $\epsilon_{\text{PE}}$ , carefully addressed in Sec. II C.

### B. Decoy-state analysis

Here, we keep the analytical decoy-state bounds provided in [12] and generalize the statistical analysis [46], assuming a common error probability  $\varepsilon$  per statistical bound for simplicity.



Table II: Decoy-state BB84 protocol inputs alien to the PE test

$T$	Number of transmission rounds
$q_X$	Test basis probability
$\mathcal{K} := \{\mu, \nu, \omega\}$	Set of intensities
$p_\mu$	Probability of setting $\mu$
$p_\nu$	Probability of setting $\nu$
$N_X$	Test data block size
$N_Z$	Key data block size
$\theta^{\text{th}}$	Threshold value for the sifted-key QBER
$\lambda_{\text{EC}}$	Error correction leakage
$\epsilon_{\text{PE}}$	Failure probability of the parameter estimation step
$\epsilon_{\text{cor}}$	Failure probability of the error correction step
$\epsilon_{\text{PA}}$	Failure probability of the privacy amplification error
$\delta$	Slack variable in the entropic chain rule [45]

The number of single-photon counts in  $\mathcal{Z}^{\text{sift}}$  is lower-bounded as

$$n_{1,Z} \stackrel{3\varepsilon}{\geq} n_{1,Z}^{\text{L}} := \frac{\tau_1 \mu}{\mu(\nu - \omega) - \nu^2 + \omega^2} \left( \frac{e^\nu}{p_\nu} n_{Z,\nu}^- - \frac{e^\omega}{p_\omega} n_{Z,\omega}^+ - \frac{\nu^2 - \omega^2}{\mu^2} \frac{e^\mu}{p_\mu} n_{Z,\mu}^+ \right), \quad (19)$$

where  $\tau_1 = \sum_{k \in \mathcal{K}} e^{-k} p_k$  and  $n_{Z,k}^\pm = B^\pm(\varepsilon, n_{Z,k}, N_Z)$  for the functions  $B^\pm(\varepsilon, n_{Z,k}, N_Z)$  of Sec. IIB 1 to Sec. IIB 4, which depend on the tail inequality under consideration for Bernoulli sampling. Importantly as well, the superscript over the inequality symbol in Eq. (19) indicates that the corresponding bound holds except with probability  $3\varepsilon$  at most. This follows from Boole's inequality [47], noticing that all three statistical estimates have error probability  $\varepsilon$  at most. We recall that this notation is extensively used below for convenience.

Complementarily to Eq. (19), it follows that

$$n_{1,Z} \stackrel{2\varepsilon}{\leq} n_{1,Z}^{\text{U}} := \tau_1 \frac{n_{Z,\nu}^+ - n_{Z,\omega}^-}{\nu - \omega}. \quad (20)$$

Replacing  $Z$  by  $X$  everywhere in Eqs. (19) and (20), we reach the corresponding bounds for the single-photon counts in  $\mathcal{X}$ ,  $n_{1,X} \stackrel{3\varepsilon}{\geq} n_{1,X}^{\text{L}}$  and  $n_{1,X} \stackrel{2\varepsilon}{\leq} n_{1,X}^{\text{U}}$ .

The number of bit errors associated with the single-photon events in  $\mathcal{X}$  is upper bounded as

$$m_{1,X} \stackrel{2\varepsilon}{\leq} m_{1,X}^{\text{U}} := \tau_1 \frac{m_{X,\nu}^+ - m_{X,\omega}^-}{\nu - \omega}, \quad (21)$$

where  $m_{X,k}^\pm = B^\pm(\varepsilon, m_{X,k}, M_X)$  and  $M_X = \sum_{k \in \mathcal{K}} m_{X,k}$ .

Lastly, it follows that

$$m_{1,X} \stackrel{3\varepsilon}{\geq} m_{1,X}^{\text{L}} := \frac{\tau_1 \mu}{\mu(\nu - \omega) - \nu^2 + \omega^2} \left( \frac{e^\nu}{p_\nu} m_{X,\nu}^- - \frac{e^\omega}{p_\omega} m_{X,\omega}^+ - \frac{\nu^2 - \omega^2}{\mu^2} \frac{e^\mu}{p_\mu} m_{X,\mu}^+ \right). \quad (22)$$

Below we provide the  $B^\pm(x, y, z)$  functions that we contemplate.

### 1. Relaxed additive Chernoff bound

First, we include the confidence intervals (CIs) that arise from our tight relaxation of the additive Chernoff bound [20]. Precisely, it follows from Proposition 1 in the main text that one can take  $B^\pm(\varepsilon, n\hat{p}, n) := n\Gamma_{n,\varepsilon}^\pm(\hat{p})$  for the statistics  $\Gamma_{n,\varepsilon}^\pm(\hat{p})$  defined therein.

### 2. Exact multiplicative Chernoff bound

Alternatively, one could follow the approach in [18], which is based on the multiplicative form of the Chernoff bound. As made explicit in [48], we have

$$B^\pm(\varepsilon, n\hat{p}, n) := n\hat{p} \pm \delta^\pm(n\hat{p}, \varepsilon), \quad (23)$$

for

$$\delta^+(x, y) = x \{W_0[-\exp(-c_{x,y})] + 1\}, \quad (24)$$

$$\delta^-(x, y) = \begin{cases} -x \{W_{-1}[-\exp(-c_{x,y})] + 1\} & \text{if } x \neq 0, \\ \ln y^{-1} & \text{if } x = 0 \end{cases}, \quad (25)$$

where  $W_j$  stands for the  $j$ -th branch of the Lambert  $W$  function and  $c_{x,y}$  is defined as  $c_{x,y} = 1 + \ln(1/y)/x$ .

### 3. Hoeffding inequality

Similarly, from Hoeffding inequality [17], we have that

$$B^\pm(\varepsilon, n\hat{p}, n) := n\hat{p} \pm \sqrt{\frac{n}{2} \ln \frac{1}{\varepsilon}}. \quad (26)$$

### 4. Exact binomial cumulative mass function

Lastly, we include the optimal CIs presented in Appendix IV, due to [30]. These rely on the exact evaluation of the binomial cumulative mass function, which is determined by the regularized beta function. Precisely, one can take

$$B^\pm(\varepsilon, n\hat{p}, n) := n [\mathcal{F}_{n,\varepsilon}^\pm(\hat{p}) \pm \Delta] \quad (27)$$

for any  $\Delta > 0$ , where the statistics  $\mathcal{F}_{n,\varepsilon}^\pm(\hat{p})$  are introduced in Theorem 1 of Appendix IV.

## C. Failure probability

In this section, we bound the failure probability of the decoy-state BB84 protocol for the different random sampling tools under consideration.

### 1. Relaxed additive Chernoff bound

In this case, the PE test is defined by the success event

$$\Omega_{\text{TEST}} = \{n_{1,Z}^L \geq n_{1,Z}^{\text{th}}, \phi_{1,Z}^U \leq \phi_{1,Z}^{\text{th}}\}, \quad (28)$$

where the threshold values  $n_{1,Z}^{\text{th}}$  and  $\phi_{1,Z}^{\text{th}}$  are the test-specific protocol inputs (see Sec. II A), the random variable  $n_{1,Z}^L$  is introduced in Sec. II B, and the random variable  $\phi_{1,Z}^U$  is defined as follows:

$$\phi_{1,Z}^U = \frac{(n_{1,Z}^U + n_{1,X}^U) \Gamma_{n_{1,X}^L, \varepsilon}^+ \left( \frac{m_{1,X}^U}{n_{1,X}^L} \right) - m_{1,X}^L}{n_{1,Z}^L}, \quad (29)$$

where the variables  $n_{1,Z}^U$ ,  $n_{1,X}^{L(U)}$  and  $m_{1,X}^{L(U)}$  are also presented in Sec. II B. Besides, we recall that  $\varepsilon > 0$  is the common error probability settled for each individual concentration inequality in Sec. II B.

On the other hand, the event where the PE thresholds are not fulfilled by the actual single-photon variables reads

$$\Omega_{\text{PE}} = \{n_{1,Z} \leq n_{1,Z}^{\text{th}}\} \cup \{\phi_{1,Z} \geq \phi_{1,Z}^{\text{th}}\}, \quad (30)$$

where  $n_{1,Z}$  stands for the number of single-photon counts in the sifted key, and  $\phi_{1,Z}$  stands for the corresponding single-photon PHER.

Given the definitions of  $\Omega_{\text{TEST}}$  and  $\Omega_{\text{PE}}$ , bounding the failure probability of the protocol amounts to finding  $\epsilon_{\text{PE}} > 0$  such that  $\Pr[\Omega_{\text{TEST}}, \Omega_{\text{PE}}] \leq \epsilon_{\text{PE}}$ . This can be easily simplified by noticing that

$$\Pr[\Omega_{\text{TEST}}, \Omega_{\text{PE}}] \leq \Pr[n_{1,Z}^L \geq n_{1,Z} \cup \phi_{1,Z}^U \leq \phi_{1,Z}], \quad (31)$$

which follows because  $A \implies B$  implies that  $\Pr[A] \leq \Pr[B]$  for arbitrary events  $A$  and  $B$ . Now, it is convenient to introduce the event where all the decoy-state bounds of Sec. II B hold. Namely,

$$\Lambda = \{n_{1,Z} \in (n_{1,Z}^L, n_{1,Z}^U), n_{1,X} \in (n_{1,X}^L, n_{1,X}^U), m_{1,X} \in (m_{1,X}^L, m_{1,X}^U)\}. \quad (32)$$

Making use of  $\Lambda$ , it follows that

$$\Pr[n_{1,Z}^L \geq n_{1,Z} \cup \phi_{1,Z}^U \leq \phi_{1,Z}] \leq \Pr[\bar{\Lambda}] + \Pr[\phi_{1,Z} \geq \phi_{1,Z}^U, \Lambda], \quad (33)$$

where we simply exploit the fact that  $\Pr[A] \leq \Pr[\bar{B}] + \Pr[A, B]$  (for arbitrary events  $A$  and  $B$ ) and further invoke the trivial implication  $\Lambda \implies n_{1,Z} > n_{1,Z}^L$ . Regarding the first term in the right-hand side of Eq. (33), carefully counting the errors in Sec. II B yields  $\Pr[\bar{\Lambda}] \leq 15\epsilon$ , and therefore we conclude

$$\Pr[\Omega_{\text{TEST}}, \Omega_{\text{PE}}] \leq 15\epsilon + \Pr[\phi_{1,Z} \geq \phi_{1,Z}^U, \Lambda]. \quad (34)$$

All that remains is to set an upper bound on  $\Pr[\phi_{1,Z} \geq \phi_{1,Z}^U, \Lambda]$ . For this, a critical observation is that

$$\Lambda \implies \phi_{1,Z}^U > q_{n_{1,Z} + n_{1,X}, n_{1,X}, \epsilon}^{\text{th}} \left( \frac{m_{1,X}}{n_{1,X}} \right), \quad (35)$$

for the threshold function  $q_{N, n, \epsilon_{\text{PE}}}^{\text{th}}(x)$  defined in Eq. (12). Crucially, note that the right-hand side in the inequality of Eq. (35) results from “dropping the superscripts” in the left-hand side (given by Eq. (29)), or equivalently, from replacing the decoy random variables  $n_{1,X(Z)}^{L(U)}$ ,  $n_{1,X(Z)}^{L(U)}$  and  $m_{1,X}^{L(U)}$  by the actual single-photon random variables  $n_{1,X(Z)}$ ,  $n_{1,X(Z)}$  and  $m_{1,X}$ . Indeed, both the definition of  $\phi_{1,Z}^U$  and the choice of  $\Lambda$  are purely ad-hoc in order to enable Eq. (35), because Proposition 2 in the main text does not apply to the decoy random variables but only to the actual single-photon random variables. In summary, because of Eq. (35),

$$\Pr[\phi_{1,Z} \geq \phi_{1,Z}^U, \Lambda] \leq \Pr\left[\phi_{1,Z} \geq q_{n_{1,Z} + n_{1,X}, n_{1,X}, \epsilon}^{\text{th}} \left( \frac{m_{1,X}}{n_{1,X}} \right)\right], \quad (36)$$

since, again,  $A \implies B$  implies that  $\Pr[A] \leq \Pr[B]$ . At this point, the only technical obstacle for the application of Proposition 2 in the main text is that this bound presumes a population with fixed size and frequency of ones (errors), and also a fixed test sample size. Therefore, by averaging over population sizes,  $n_{1,Z} + n_{1,X}$ , test sample sizes,  $n_{1,X}$ , and total frequencies of errors,  $(m_{1,Z}^{\text{ph}} + m_{1,X})/(n_{1,Z} + n_{1,X})$ —where we have introduced  $m_{1,Z}^{\text{ph}} = \phi_{1,Z} n_{1,Z}$  for clarity—, Proposition 2 in the main text applies for each individual term in the average and, therefore,

$$\Pr\left[\phi_{1,Z} \geq q_{n_{1,Z} + n_{1,X}, n_{1,X}, \epsilon}^{\text{th}} \left( \frac{m_{1,X}}{n_{1,X}} \right)\right] \leq \epsilon \quad (37)$$

follows. Note that this averaging technique is of the exact same nature as the one used to bound the failure probability of the BBM92 protocol (Proposition 3 in the main text), also deployed in [8, 15]. Lastly, combining this bound with Eqs. (36) and (34), we reach  $\Pr[\Omega_{\text{TEST}}, \Omega_{\text{PE}}] \leq 16\epsilon$ . In conclusion, with the random sampling tool proposed in this work,  $\epsilon_{\text{PE}} = 16\epsilon$  provides the desired upper bound on the failure probability.

## 2. Serfling and Hush & Scovel inequalities combined

The result in [15] is devised for the ideal BBM92 protocol, and it is a side contribution of this work to make it compatible with the practical decoy-state BB84 protocol. For this purpose, the alternative PE test we consider is

$$\Omega_{\text{TEST}} = \left\{ n_{1,Z}^L \geq n_{1,Z}^{\text{th},L}, n_{1,Z}^U \leq n_{1,Z}^{\text{th},U}, n_{1,X}^L \geq n_{1,X}^{\text{th},L}, n_{1,X}^U \leq n_{1,X}^{\text{th},U}, m_{1,X}^U \leq m_{1,X}^{\text{th},U} \right\}, \quad (38)$$

where the threshold values  $n_{1,Z}^{\text{th},L(U)}$ ,  $n_{1,X}^{\text{th},L(U)}$  and  $m_{1,X}^{\text{th},U}$  are the test-specific protocol inputs (see Sec. II A). On the other hand, the event where the PE thresholds do not hold is again given by  $\Omega_{\text{PE}} = \{n_{1,Z} \leq n_{1,Z}^{\text{th}}\} \cup \{\phi_{1,Z} \geq \phi_{1,Z}^{\text{th}}\}$ , recalling that, in this case,  $n_{1,Z}^{\text{th}}$  and  $\phi_{1,Z}^{\text{th}}$  are defined in Eq. (17) in terms of the thresholds above.

We now introduce the event

$$\Sigma = \{n_{1,Z} \in (n_{1,Z}^L, n_{1,Z}^U), n_{1,X} \in (n_{1,X}^L, n_{1,X}^U), m_{1,X} < m_{1,X}^U\}, \quad (39)$$

which matches  $\Lambda$  in Eq. (32) exactly except from the fact that it does not contemplate the condition  $\{m_{1,X} > m_{1,X}^L\}$ . In particular, this implies that  $\Pr[\bar{\Sigma}] = 12\varepsilon$  (composing the relevant errors in Sec. II C), and therefore  $\Pr[\Omega_{\text{TEST}}, \Omega_{\text{PE}}] \leq 12\varepsilon + \Pr[\Omega_{\text{TEST}}, \Omega_{\text{PE}}, \Sigma]$ . Crucially at this point, the ad hoc definitions of  $\Omega_{\text{TEST}}$  and  $\Sigma$  assure the following trivial implications:

$$\begin{aligned} (\Omega_{\text{TEST}}, \Sigma) &\implies \left\{ n_{1,Z(X)} \in (n_{1,Z(X)}^{\text{th},L}, n_{1,Z(X)}^{\text{th},U}), m_{1,X} < m_{1,X}^{\text{th},U} \right\} \implies \\ &\left\{ e_{1,X} \leq e_{1,X}^{\text{th}}, \phi_{1,Z}^{\text{th}} \geq q_{n_{1,Z} + n_{1,X}, n_{1,X}, \varepsilon}^{\text{th}}(e_{1,X}^{\text{th}}) \right\}, \end{aligned} \quad (40)$$

where we have introduced the single-photon bit-error rate  $e_{1,X} = m_{1,X}/n_{1,X}$ . Namely, the conjunction of  $\Omega_{\text{TEST}}$  and  $\Sigma$  guarantees that the actual single-photon variables—and not only their decoy-state bounds—fulfil the thresholds of the PE test (first implication in Eq. (40)), which in turn implies that the random variable  $e_{1,X} = m_{1,X}/n_{1,X}$  is upper-bounded by the value  $e_{1,X}^{\text{th}} = m_{1,X}^{\text{th},U}/n_{1,X}^{\text{th},L}$ , and the value  $\phi_{1,Z}^{\text{th}} = \max_{u,v \in \mathcal{B}} q_{u,v, \varepsilon_{\text{PE}}}^{\text{th}}(e_{1,X}^{\text{th}})$  is equal or larger than the function of random variables  $q_{n_{1,Z} + n_{1,X}, n_{1,X}, \varepsilon}^{\text{th}}(e_{1,X}^{\text{th}})$  (second implication in Eq. (40)). The latter holds simply because, if the actual single-photon RVs  $n_{1,Z}$  and  $n_{1,X}$  fulfil the thresholds of the PE test, the threshold function evaluated in these variables cannot be larger than the threshold function evaluated in the worst-case variables compatible with the thresholds (captivated by the maximization of some arbitrary inputs  $u$  and  $v$  over  $\mathcal{B}$ ).

In short, we have

$$\begin{aligned} \Pr[\Omega_{\text{TEST}}, \Omega_{\text{PE}}, \Sigma] &\leq \Pr\left[n_{1,Z(X)} \in (n_{1,Z(X)}^{\text{th},L}, n_{1,Z(X)}^{\text{th},U}), m_{1,X} < m_{1,X}^{\text{th},U}, \phi_{1,Z} \geq \phi_{1,Z}^{\text{th}}\right] \\ &\leq \Pr\left[e_{1,X} \leq e_{1,X}^{\text{th}}, \phi_{1,Z}^{\text{th}} \geq q_{n_{1,Z} + n_{1,X}, n_{1,X}, \varepsilon}^{\text{th}}(e_{1,X}^{\text{th}}), \phi_{1,Z} \geq \phi_{1,Z}^{\text{th}}\right] \\ &\leq \Pr\left[e_{1,X} \leq e_{1,X}^{\text{th}}, \phi_{1,Z} \geq q_{n_{1,Z} + n_{1,X}, n_{1,X}, \varepsilon}^{\text{th}}(e_{1,X}^{\text{th}})\right], \end{aligned} \quad (41)$$

where in the first inequality we invoke the first implication of Eq. (40)—and disregard the event  $n_{1,Z} \leq n_{1,Z}^{\text{th}}$  of  $\Omega_{\text{PE}}$  because it is incompatible with  $n_{1,Z} \in (n_{1,Z}^{\text{th},L}, n_{1,Z}^{\text{th},U})$ —, in the second inequality we invoke the second implication of Eq. (40), and in the third inequality we make use of the fact that  $\left\{ \phi_{1,Z}^{\text{th}} \geq q_{n_{1,Z} + n_{1,X}, n_{1,X}, \varepsilon}^{\text{th}}(e_{1,X}^{\text{th}}), \phi_{1,Z} \geq \phi_{1,Z}^{\text{th}} \right\} \implies \left\{ \phi_{1,Z} \geq q_{n_{1,Z} + n_{1,X}, n_{1,X}, \varepsilon}^{\text{th}}(e_{1,X}^{\text{th}}) \right\}$ . To finish with, the desired bound follows from an averaging technique, as usual. Particularly, averaging over population sizes  $(n_{1,Z} + n_{1,X})$  and test sample sizes  $(n_{1,X})$  in this case, it follows that

$$\Pr\left[e_{1,X} \leq e_{1,X}^{\text{th}}, \phi_{1,Z} \geq q_{n_{1,Z} + n_{1,X}, n_{1,X}, \varepsilon}^{\text{th}}(e_{1,X}^{\text{th}})\right] \leq \varepsilon \quad (42)$$

from the random sampling bound derived in [15]. Putting it all together, we reach  $\Pr[\Omega_{\text{TEST}}, \Omega_{\text{PE}}] \leq 13\varepsilon$ , and thus we can take  $\varepsilon_{\text{PE}} = 13\varepsilon$ .

### 3. Serfling inequality

With this tool [8, 14], we define the PE test of the protocol equally as in Sec. II C 1, but taking

$$\phi_{1,Z}^U = \frac{m_{1,X}^U}{n_{1,X}^L} + \sqrt{\frac{(n_{1,Z}^U + n_{1,X}^U)(n_{1,X}^U + 1) \ln(\varepsilon^{-1})}{2n_{1,Z}^L (n_{1,X}^L)^2}}. \quad (43)$$

Namely, we use the threshold function of Eq. (15) rather than that of Eq. (12). In these circumstances, one can readily prove the failure probability bound  $\varepsilon_{\text{PE}} = 13\varepsilon$  reproducing the steps of Sec. II C 1, but with the ancillary event  $\Sigma$  (Eq. (39)) rather than  $\Lambda$  (Eq. (32)). This analogy with Sec. II C 1 comes from the fact that the bound based on Serfling inequality can be trivially stated in the form of Proposition 2 in the main text, just like the bound proposed in this work.

#### 4. Exact hypergeometric cumulative mass function

Similarly, the bound based on the Clopper-Pearson method [19, 27] can be stated in the form of Proposition 2 in the main text too. As a consequence, considering the simple PE test of Sec. II C 1, one can establish that  $\epsilon_{\text{PE}} = 16\epsilon$  following the exact same steps presented there—in particular, keeping the ancillary event  $\Lambda$  of Eq. (32)—, but taking

$$\phi_{1,Z}^{\text{U}} = \frac{(n_{1,Z}^{\text{U}} + n_{1,X}^{\text{U}}) \mathcal{CP}_{n_{1,Z}^{\text{U}} + n_{1,X}^{\text{U}}, n_{1,X}^{\text{L}}, \varepsilon}^+ \left( \frac{m_{1,X}^{\text{U}}}{n_{1,X}^{\text{L}}} \right) - m_{1,X}^{\text{L}}}{n_{1,Z}^{\text{L}}}. \quad (44)$$

#### D. Channel model

Here, we describe the detector and channel model deployed in the decoy-state BB84 simulations of the main text. The expected detection rate of a signal of intensity  $k$  is given by

$$D_k = 1 - (1 - 2p_d) \exp(-\eta k), \quad (45)$$

and the probability of having a bit error for intensity  $k$  is given by

$$e_k = p_d + e_{\text{mis}} [1 - \exp(-\eta k)], \quad (46)$$

where  $p_d$  is the dark count probability of Bob's detectors,  $e_{\text{mis}}$  is the misalignment error rate of the system, and  $\eta$  is the overall system efficiency. Namely,  $\eta = 10^{-\lambda/10}$ ,  $\lambda$  denoting the total loss in dB.

This model is used to select the threshold values of the PE test. To be precise, the thresholds are set to the expectation values of the underlying variables according to the channel model. As an example, within the PE test  $\Omega_{\text{TEST}} = \{n_{1,Z}^{\text{L}} \geq n_{1,Z}^{\text{th}}, \phi_{1,Z}^{\text{U}} \leq \phi_{1,Z}^{\text{th}}\}$ ,  $n_{1,Z}^{\text{th}}$  is set to the decoy-state bound of Eq. (19), upon replacement of  $n_{Z,k}$  by its expectation according to the channel model:

$$E[n_{Z,k}] = N_Z \frac{p_k D_k}{\sum_j p_j D_j}. \quad (47)$$

Similarly,  $\phi_{1,Z}^{\text{th}}$  is set to the threshold function under consideration, upon replacement of all the observables ( $n_{Z,k}$ ,  $n_{X,k}$  and  $m_{X,k}$ ) by their expectations according to the channel model. Particularly,

$$E[m_{X,k}] = N_X \frac{p_k e_k}{\sum_j p_j D_j}, \quad (48)$$

and  $E[n_{X,k}]$  is obtained simply replacing  $Z$  by  $X$  in Eq. (47).

We remark that the above choices of the thresholds in the PE test are over-optimistic, as they would incur in large abortion probabilities even if the channel behaves according to the considered model [49]. A more sensitive approach consists of making robustness considerations to incorporate statistical fluctuations in the thresholds. Ultimately, however, in a real experiment, the thresholds would be chosen via careful channel monitoring.

### APPENDIX III: COMPUTING CONFIDENCE INTERVALS FROM THE ADDITIVE CHERNOFF BOUNDS

This section includes the technical derivations underlying Proposition 1 in the main text. In the first place, we provide a relaxation of the upper additive Chernoff bound [20].

**Proposition 4.** *Let  $\hat{p}$  be the average of  $n$  independent Bernoulli variables, with expected value  $\mathbb{E}(\hat{p}) = p$ . Then, for all  $z \in [p, 1]$ ,  $\Pr[\hat{p} \geq z] \leq e^{-nD(z,p)}$  for  $D(z,p) = 9(z-p)^2/2(z+2p)(3-z-2p)$ .*

*Proof.* We recall that the original bound [20] is analogous to the above proposition but replacing  $D(z,p)$  by the Kullback-Leibler divergence,

$$D(z||p) = z \ln \left( \frac{z}{p} \right) + (1-z) \ln \left( \frac{1-z}{1-p} \right). \quad (49)$$



Plugging the logarithmic inequality  $\ln(1+z) \geq z(6+5z)/2(1+z)(3+z)$  [24] in each term of the divergence yields

$$D(z||p) \geq z \frac{(\frac{z}{p}-1)(6+5(\frac{z}{p}-1))}{2(1+(\frac{z}{p}-1))(3+(\frac{z}{p}-1))} + (1-z) \frac{(\frac{1-z}{1-p}-1)(6+5(\frac{1-z}{1-p}-1))}{2(1+(\frac{1-z}{1-p}-1))(3+(\frac{1-z}{1-p}-1))}, \quad (50)$$

which, after some straightforward manipulation, leads to

$$D(z||p) \geq \frac{(z-p)(p+5z)}{2(z+2p)} + \frac{(p-z)(6-5z-p)}{2(3-z-2p)}. \quad (51)$$

Lastly, combining both summands in a single fraction and simplifying yields

$$D(z||p) \geq \frac{9(z-p)^2}{2(z+2p)(3-z-2p)} =: D(z, p) \quad (52)$$

Hence, the desired relaxation follows.  $\square$

Coming next, we reformulate Proposition 1 above to determine the upper bound on  $\hat{p}$  that matches any desired error probability  $\epsilon$ .

**Proposition 5.** *Let  $\hat{p}$  be the average of  $n$  independent Bernoulli variables, with expected value  $\mathbb{E}(\hat{p}) = p$  such that  $p \leq (1-2\kappa_{n,\epsilon})/(1+4\kappa_{n,\epsilon})$  for  $\kappa_{n,\epsilon} = (2/9n) \ln(1/\epsilon)$ . Then,  $\Pr[\hat{p} \geq z_{n,\epsilon}(p)] \leq \epsilon$  with*

$$z_{n,\epsilon}(p) = \frac{-b_{n,\epsilon}(p) + \sqrt{b_{n,\epsilon}(p)^2 - 4a_{n,\epsilon}c_{n,\epsilon}(p)}}{2a_{n,\epsilon}}, \quad (53)$$

where  $a_{n,\epsilon} = 1 + \kappa_{n,\epsilon}$ ,  $b_{n,\epsilon}(p) = -2p - \kappa_{n,\epsilon}(3-4p)$  and  $c_{n,\epsilon}(p) = p^2 - \kappa_{n,\epsilon}p(6-4p)$ .

*Proof.* According to Proposition 1, for all  $z \in [p, 1]$ ,  $\Pr[\hat{p} \geq z] \leq \epsilon$  holds if  $\epsilon = \exp\{-nD(z, p)\}$ . Let us consider the function  $g_{n,p}(z) = \exp\{-nD(z, p)\}$  that maps  $z$ 's to  $\epsilon$ 's for arbitrary  $n$  and  $p$ . Since  $g_{n,p}(z)$  is decreasing and thus injective in  $[p, 1]$ , it admits an inverse in  $g_{n,p}([p, 1]) = [g_{n,p}(1), 1]$ . Namely, for all  $\epsilon \geq g_{n,p}(1)$ ,  $\Pr[\hat{p} \geq z] \leq \epsilon$  holds if  $z = g_{n,p}^{-1}(\epsilon)$ , which is the only  $z \in [p, 1]$  such that  $g_{n,p}(z) = \epsilon$ . This is a quadratic equation  $a_{n,\epsilon}z^2 + b_{n,\epsilon}(p)z + c_{n,\epsilon}(p) = 0$  with the coefficients prescribed in the statement, and one can readily show that only the larger root lies in  $[p, 1]$ . Lastly, the claim follows by observing that  $\epsilon \geq g_{n,p}(1) \Leftrightarrow p \leq (1-2\kappa_{n,\epsilon})/(1+4\kappa_{n,\epsilon})$  [50].  $\square$

Let us now use Proposition 2 to infer a one-sided CI for the underlying parameter  $p$  [51, 52]. Analytical inspection shows that  $z_{n,\epsilon}(p)$  is monotonically increasing in the interval  $[0, (1-2\kappa_{n,\epsilon})/(1+4\kappa_{n,\epsilon})]$ , and thus it admits an inverse  $z_{n,\epsilon}^{-1}$  in  $I_{n,\epsilon} = z_{n,\epsilon}([0, (1-2\kappa_{n,\epsilon})/(1+4\kappa_{n,\epsilon})]) = [3\kappa_{n,\epsilon}/(1+\kappa_{n,\epsilon}), 1]$ . By definition,  $z_{n,\epsilon}^{-1}(x)$  is the only  $p < x$  such that  $z_{n,\epsilon}(p) = x$ . Solving this quadratic equation for  $p$  and choosing the relevant root we conclude that, for all  $x \in [3\kappa_{n,\epsilon}/(1+\kappa_{n,\epsilon}), 1]$ ,

$$z_{n,\epsilon}^{-1}(x) = \frac{1}{1+4\kappa_{n,\epsilon}} \left( 3\kappa_{n,\epsilon} + (1-2\kappa_{n,\epsilon})x - 3\sqrt{\kappa_{n,\epsilon}(\kappa_{n,\epsilon} + x - x^2)} \right). \quad (54)$$

Essentially,  $z_{n,\epsilon}^{-1}(\hat{p})$  is the statistic we use to construct a CI on  $p$ , as shown next.

**Proposition 6.** *Let  $\hat{p}$  be the average of  $n$  independent Bernoulli variables, with expected value  $\mathbb{E}[\hat{p}] = p$ . Then, for all  $\epsilon > 0$ ,  $\Pr[\Gamma_{n,\epsilon}^-(\hat{p}) \geq p] \leq \epsilon$ , where  $\Gamma_{n,\epsilon}^-(\hat{p}) = z_{n,\epsilon}^{-1}(\hat{p})$  if  $\hat{p} \in I_{n,\epsilon}$ , and  $\Gamma_{n,\epsilon}^-(\hat{p}) = -\epsilon$  otherwise.*

*Proof.* For all  $\hat{p}$ ,  $\Gamma_{n,\epsilon}^-(\hat{p}) \leq \Gamma_{n,\epsilon}^-(1) = (1-2\kappa_{n,\epsilon})/(1+4\kappa_{n,\epsilon})$ . Hence, the claim holds if  $(1-2\kappa_{n,\epsilon})/(1+4\kappa_{n,\epsilon}) < p \leq 1$ . Let us now consider  $0 \leq p \leq (1-2\kappa_{n,\epsilon})/(1+4\kappa_{n,\epsilon})$ . We have  $\Pr[\Gamma_{n,\epsilon}^-(\hat{p}) \geq p] = \Pr[\hat{p} \in I_{n,\epsilon}, \Gamma_{n,\epsilon}^-(\hat{p}) \geq p] = \Pr[\hat{p} \in I_{n,\epsilon}, z_{n,\epsilon}^{-1}(\hat{p}) \geq p] \leq \Pr[\hat{p} \in I_{n,\epsilon}, \hat{p} \geq z_{n,\epsilon}(p)] \leq \Pr[\hat{p} \geq z_{n,\epsilon}(p)] \leq \epsilon$ . Here, the first equality follows because  $\hat{p} \notin I_{n,\epsilon} \Rightarrow \Gamma_{n,\epsilon}^-(\hat{p}) = -\epsilon < p$  [53], the second equality follows because  $\hat{p} \in I_{n,\epsilon} \Rightarrow \Gamma_{n,\epsilon}^-(\hat{p}) = z_{n,\epsilon}^{-1}(\hat{p})$ , the first inequality follows because  $\{\hat{p} \in I_{n,\epsilon}, z_{n,\epsilon}^{-1}(\hat{p}) \geq p\} \Rightarrow \{\hat{p} \in I_{n,\epsilon}, \hat{p} \geq z_{n,\epsilon}(p)\}$  —as  $z_{n,\epsilon}^{-1}(\hat{p})$  is monotonically increasing in  $I_{n,\epsilon}$ —, the second inequality follows because  $\{\hat{p} \in I_{n,\epsilon}, \hat{p} \geq z_{n,\epsilon}(p)\} \Rightarrow \{\hat{p} \geq z_{n,\epsilon}(p)\}$ , and the final inequality follows from Proposition 2 above.  $\square$

We remark that, ultimately, propositions 1 to 3 originate from the upper additive Chernoff bound. Importantly, for each of them, there exists an analogous statement arising from the lower additive Chernoff bound instead. In particular, a one-sided CI complementary to that of Proposition 3 follows.

**Proposition 7.** Let  $\hat{p}$  be the average of  $n$  independent Bernoulli variables, with expected value  $\mathbb{E}(\hat{p}) = p$ . Then, for all  $\epsilon > 0$ ,  $\Pr[\Gamma_{n,\epsilon}^+(\hat{p}) \leq p] \leq \epsilon$ , where

$$\Gamma_{n,\epsilon}^+(\hat{p}) = \frac{1}{1 + 4\kappa_{n,\epsilon}} \left( 3\kappa_{n,\epsilon} + (1 - 2\kappa_{n,\epsilon})\hat{p} + 3\sqrt{\kappa_{n,\epsilon}(\kappa_{n,\epsilon} + \hat{p} - \hat{p}^2)} \right) \quad (55)$$

if  $\hat{p} \in [0, (1 - 2\kappa_{n,\epsilon})/(1 + \kappa_{n,\epsilon})]$ , and  $\Gamma_{n,\epsilon}^+(\hat{p}) = 1 + \epsilon$  otherwise.

*Proof.* The proof follows similar lines as that of Proposition 3 above, but using the lower additive Chernoff bound as the starting point.  $\square$

Proposition 1 in the main text is the conjunction of propositions 3 and 4 presented here.

#### APPENDIX IV: OPTIMAL CONFIDENCE INTERVALS FOR THE AVERAGE PARAMETER OF A SET OF INDEPENDENT BERNOULLI VARIABLES

Here, we present the tightest monotonic one-sided CIs for the average parameter of a set of independent Bernoulli variables [54–56], originally derived in [30].

**Theorem 1.** Let  $\hat{p}$  be the average of  $n$  independent Bernoulli variables, with expected value  $\mathbb{E}[\hat{p}] = p$ . Then, for all  $\epsilon \in (0, 1/4]$ , we have that  $\Pr[\mathcal{F}_{n,\epsilon}^-(\hat{p}) > p] \leq \epsilon$  for

$$\mathcal{F}_{n,\epsilon}^-(\hat{p}) = \begin{cases} 0 & \text{if } n\hat{p} = 0, \\ \hat{p} - \frac{1 - \epsilon}{n[1 - \epsilon^*(n\hat{p}, n)]} & \text{if } n\hat{p} > 0, \quad \epsilon^*(n\hat{p}, n) \leq \epsilon \leq 1, \\ I_\epsilon^{-1}(n\hat{p}, n - n\hat{p} + 1) & \text{if } n\hat{p} > 0, \quad 0 \leq \epsilon \leq \epsilon^*(n\hat{p}, n), \end{cases} \quad (56)$$

where  $\epsilon^*(n\hat{p}, n) = I_{(n\hat{p}-1)/n}(n\hat{p}, n - n\hat{p} + 1)$  and  $I_\epsilon^{-1}(a, b)$  denotes the inverse regularized incomplete beta function, such that  $I_{I_\epsilon^{-1}(a,b)}(a, b) = \epsilon$  for

$$I_x(a, b) = \frac{\int_0^x t^{a-1}(1-t)^{b-1} dt}{\int_0^1 t^{a-1}(1-t)^{b-1} dt}. \quad (57)$$

Complementarily, for all  $\epsilon \in (0, 1/4]$ , we have that  $\Pr[\mathcal{F}_{n,\epsilon}^+(\hat{p}) < p] \leq \epsilon$  for  $\mathcal{F}_{n,\epsilon}^+(\hat{p}) = 1 - \mathcal{F}_{n,\epsilon}^-(1 - \hat{p})$ .

To finish with, two observations are in order. On the one hand, note that for any  $\Delta > 0$ ,  $\{\mathcal{F}_{n,\epsilon}^-(\hat{p}) \geq p + \Delta\} \implies \{\mathcal{F}_{n,\epsilon}^-(\hat{p}) > p\}$ , such that  $\Pr[\mathcal{F}_{n,\epsilon}^-(\hat{p}) \geq p + \Delta] = \Pr[(\mathcal{F}_{n,\epsilon}^-(\hat{p}) - \Delta) \geq p] \leq \epsilon$  in virtue of Theorem 1. In other words, by decreasing  $\mathcal{F}_{n,\epsilon}^-(\hat{p})$  in any nonzero amount  $\Delta$ , we reach a looser lower bound that trivially sticks to the sign convention used in this work, *i.e.* contemplating the equality sign in the probability (rather than the strict inequality considered in Theorem 1). Similarly, increasing  $\mathcal{F}_{n,\epsilon}^+(\hat{p})$  in any nonzero amount allows to meet the desired criterion for the upper bound.

On another note, binomial-like CIs slightly simpler than those of Theorem 1 are provided in [57], which only entail a trivial loss of optimality imperceptible with the sample sizes characteristic of QKD applications.

- 
- [1] Portmann, C. & Renner, R. Security in quantum cryptography. *Reviews of Modern Physics* **94**, 025008 (2022).
  - [2] Xu, F., Ma, X., Zhang, Q., Lo, H.-K. & Pan, J.-W. Secure quantum key distribution with realistic devices. *Reviews of Modern Physics* **92**, 025002 (2020).
  - [3] Lo, H.-K., Curty, M. & Tamaki, K. Secure quantum key distribution. *Nature Photonics* **8**, 595-604 (2014).
  - [4] Bennett, C. H. & Brassard, G. Quantum cryptography: public key distribution and coin tossing. In *Proceedings IEEE International Conference on Computers, Systems & Signal Processing*, 175–179 (IEEE, NY, Bangalore, India, 1984).
  - [5] Tomamichel, M. & Renner, R. Uncertainty relation for smooth entropies. *Physical Review Letters* **106**, 110506 (2011).
  - [6] Coles, Patrick J., *et al.* Entropic uncertainty relations and their applications. *Reviews of Modern Physics* **89**, 015002 (2017).

- [7] Bennett, C. H., Brassard, G. & Mermin, M. D. Quantum cryptography without Bell’s theorem. *Physical Review Letters* **68**, 557 (1992).
- [8] Tomamichel, M. & Leverrier, A. A largely self-contained and complete security proof for quantum key distribution. *Quantum* **1**, 14 (2017).
- [9] Hwang, W. Y. Quantum key distribution with high loss: toward global secure communication. *Physical Review Letters* **91**, 057901 (2003).
- [10] Lo, H.-K., Ma, X. & Chen, K. Decoy state quantum key distribution. *Physical Review Letters* **94**, 230504 (2005).
- [11] Wang, X.-B. Beating the photon-number-splitting attack in practical quantum cryptography. *Physical Review Letters* **94**, 230503 (2005).
- [12] Lim, C. C. W., Curty, M., Walenta, N., Xu, F. & Zbinden, H. Concise security bounds for practical decoy-state quantum key distribution. *Physical Review A* **89**, 022307 (2014).
- [13] Tomamichel, M., Lim, C. C. W., Gisin, N. & Renner, R. Tight finite-key analysis for quantum cryptography. *Nature Communications* **3**, 1-6 (2012).
- [14] Serfling, R. J. Probability inequalities for the sum in sampling without replacement. *The Annals of Statistics* **2**, 39-48 (1974).
- [15] Lim, C. C. W., Xu, F., Pan, J. W., & Ekert, A. Security analysis of quantum key distribution with small block length and its application to quantum space communications. *Physical Review Letters* **126**, 100501 (2021).
- [16] Hush, D., & Scovel, C. Concentration of the hypergeometric distribution. *Statistics & Probability Letters* **75**, 127-132 (2005).
- [17] Hoeffding, W. Probability inequalities for sums of bounded random variables. *Journal of the American Statistical Association* **58**, 13-30 (1963).
- [18] Zhang, Z., Zhao, Q., Razavi, M., & Ma, X. Improved key-rate bounds for practical decoy-state quantum-key-distribution systems. *Physical Review A* **95**, 012333 (2017).
- [19] Clopper, C. J., & Pearson, E. S. The use of confidence or fiducial limits illustrated in the case of the binomial. *Biometrika* **26**, 404-413 (1934).
- [20] Chernoff, H. A measure of asymptotic efficiency for tests of a hypothesis based on the sum of observations. *The Annals of Mathematical Statistics* **23**, 493-507 (1952).
- [21] Chvátal, V. The tail of the hypergeometric distribution. *Discrete Mathematics* **25**, 285-287 (1979).
- [22] Hayashi, M., & Tsurumaru, T. Concise and tight security analysis of the Bennett–Brassard 1984 protocol with finite key lengths. *New Journal of Physics* **14**, 093014 (2012).
- [23] Hayashi, M., & Nakayama, R. Security analysis of the decoy method with the Bennett–Brassard 1984 protocol for finite key lengths. *New Journal of Physics* **16**, 063009 (2014).
- [24] Topsøe, F. Some bounds for the logarithmic function. *Inequality Theory and Applications* **4**, 137 (Nova Publishers, 2007).
- [25] For instance, it is straightforward to show that setting  $\epsilon > \exp\left(-\frac{9(N-n)n}{4(2n+N)}\right)$  suffices to assure that  $\Gamma_{n,\epsilon}^{+'}(p^{\text{th}}) \geq n/N$  for all  $p^{\text{th}} < 1/2$ . This condition on  $\epsilon$  is unrestrictive for all practical purposes.
- [26] Buonaccorsi, J. P. A note on confidence intervals for proportions in finite populations. *The American Statistician* **41**, 215-218 (1987).
- [27] Wright, T. *Exact confidence bounds when sampling from small finite universes: an easy reference based on the hypergeometric distribution* (Springer Science & Business Media, Vol. 66, 2012).
- [28] The statistic  $\mathcal{CP}_{N,n,\epsilon}^{+}(\hat{p})$  we introduce here does not exactly match—but is trivially determined by—the one presented in [27]. Particularly, they are related by a “one-unit shift”, and the discrepancy arises because we request  $\Pr[\mathcal{CP}_{N,n,\epsilon}^{+}(\hat{p}) \leq p] \leq \epsilon$  rather than  $\Pr[\mathcal{CP}_{N,n,\epsilon}^{+}(\hat{p}) < p] \leq \epsilon$ .
- [29] One can speed-up the computation of  $\mathcal{CP}_{N,n,\epsilon}^{+}(x)$  by exploring the complementary set of potential  $p$ ’s (namely,  $\{p \geq x \mid \Pr[\hat{p} \leq x|p] > \epsilon\}$ ), by carefully selecting the starting  $p$  for the iterations (e.g. based on existing analytical bounds), or by applying a binary search/interpolation algorithm.
- [30] Bancal, J. D., & Sekatski, P. Simple Buehler-optimal confidence intervals on the average success probability of independent Bernoulli trials. arXiv preprint arXiv:2212.12558 (2022).
- [31] Mattner, L., & Tasto, C. Confidence intervals for average success probabilities. arXiv preprint arXiv:1403.0229 (2014).
- [32] Lucamarini, M. *et al.* Efficient decoy-state quantum key distribution with quantified security. *Optics Express* **21**, 24550-24565 (2013).
- [33] Lucamarini, M., Dynes, J. F., Fröhlich, B., Yuan, Z., & Shields, A. J. Security bounds for efficient decoy-state quantum key distribution. *IEEE Journal of Selected Topics in Quantum Electronics* **21**, 197-204 (2015).
- [34] Yin, J., *et al.* Entanglement-based secure quantum cryptography over 1,120 kilometres. *Nature* **582**, 501-505 (2020).
- [35] Curty, M., Xu, F., Cui, W., Lim, C. C. W., Tamaki, K., Lo, H.-K. Finite-key analysis for measurement-device-independent quantum key distribution. *Nature Communications* **5**, 3732 (2014).
- [36] A novelty of our protocol with respect to [12] is that, in the PE step, the parties evaluate suitable decoy-state bounds for the single-photon security parameters (*e.g.* the number of single-photon counts and their PHER). If these bounds do not fulfill predetermined acceptance thresholds, the protocol aborts. Otherwise, a fixed-length output key matching the acceptance thresholds is extracted. Furthermore, a finer-grained PE test is devised when considering the tool of [15], in order to adapt this tool to the decoy-state setting. This is explained in Supplemental Material II.
- [37] Walenta, N., *et al.* Sine gating detector with simple filtering for low-noise infra-red single photon detection at room temperature. *Journal of Applied Physics* **112**, 063106 (2012).

- [38] Note that  $\theta^{\text{th}}$  here differs from the threshold single-photon error rate of the BBM92 protocol,  $p^{\text{th}}$ . For consistency,  $\theta^{\text{th}}$  is set to the expected QBER of the considered channel model.
- [39] The total number of error terms contributing to  $\epsilon_{\text{PE}}$  varies depending on the random sampling tool under consideration, and the reader is referred to Supplemental Material II for the details.
- [40] Sidhu, J. S., Brougham, T., McArthur, D., Pousa, R. G. & Oi, D. K. Finite key effects in satellite quantum key distribution. *npj Quantum Information* **8**, 18 (2022).
- [41] Roger, T., *et al.* Real-time gigahertz free-space quantum key distribution within an emulated satellite overpass. *Science Advances* **9**, eadj5873 (2023).
- [42] Bedington, R., Arrazola, J. M. & Ling, A. Progress in satellite quantum key distribution. *npj Quantum Information* **3**, 30 (2017).
- [43] Tomamichel, M., *et al.* Leftover hashing against quantum side information. *IEEE Transactions on Information Theory* **57**, 5524-5535 (2011).
- [44] Zapatero, V., & Curty, M. Finite-key security of passive quantum key distribution. *Physical Review Applied* **21**, 014018 (2024).
- [45] Vitanov, A., *et al.* Chain rules for smooth min-and max-entropies. *IEEE Transactions on Information Theory* **59**, 2603-2612 (2013).
- [46] A relevant observation is that, in order to enable the counterfactual argument given in [12] (on which the finite statistical analysis is based), we assume that the intensity assignments are performed only after the data sampling.
- [47] Bonferroni, C. Teoria statistica delle classi e calcolo delle probabilita. *Pubblicazioni del R istituto superiore di scienze economiche e commerciali di firenze* **8**, 3-62 (1936).
- [48] Zapatero, V., & Curty, M. Secure quantum key distribution with a subset of malicious devices. *npj Quantum Information*, **7(1)**, 26 (2021).
- [49] In fact, strictly speaking, the “robustness” penalty of using these thresholds is critical when considering the more convoluted PE test devised for the random sampling tool of [15]. This is so because, in that test, double-sided thresholds are imposed, and since both the upper and the lower thresholds are being set to the same value for the simulations, the success probability of the test becomes negligible.
- [50] Note that the bound becomes identically trivial if  $\kappa_{n,\epsilon} > 1/2$ . Nevertheless, practical situations are typically far away from this very extreme regime.
- [51] Neyman, J. On the problem of confidence intervals. *The Annals of Mathematical Statistics* **6**, 111-116 (1936).
- [52] Neyman, J. Outline of a theory of statistical estimation based on the classical theory of probability. *Philosophical Transactions of the Royal Society of London. Series A, Mathematical and Physical Sciences* **236**, 333-380 (1937).
- [53] Note that the equality sign in the probability  $\Pr[\Gamma_{n,\epsilon}^-(\hat{p}) \geq p]$  prevents us from defining  $\Gamma_{n,\epsilon}^-(\hat{p}) = 0$  directly for  $\hat{p} \notin I_{n,\epsilon}$ . In particular, let  $\Upsilon_{n,\epsilon}^-(\hat{p})$  follow this alternative definition. Then, if  $p = 0$ , for sure  $\hat{p} = 0 \notin I_{n,\epsilon}$  and hence  $\Upsilon_{n,\epsilon}^-(\hat{p}) = 0$ , such that  $\Pr[\Upsilon_{n,\epsilon}^-(\hat{p}) \geq p] = \Pr[\Upsilon_{n,\epsilon}^-(\hat{p}) = p] = 1 > \epsilon$ .
- [54] This notion of optimality is sometimes referred to as Buehler-optimality [55, 56].
- [55] Buehler, R. J. Confidence intervals for the product of two binomial parameters. *Journal of the American Statistical Association* **52**, 482-493 (1957).
- [56] Lloyd, C. J., & Kabaila, P. On the optimality and limitations of Buehler bounds. *Australian & New Zealand Journal of Statistics* **45**, 167-174 (2003).
- [57] Bancal, J. D., Redeker, K., Sekatski, P., Rosenfeld, W., & Sangouard, N. Self-testing with finite statistics enabling the certification of a quantum network link. *Quantum* **5**, 401 (2021).